AUXILIARY MATERIAL FOR

COMPLEMENTING THERMOSTERIC SEA LEVEL RISE ESTIMATES

BY KATJA LORBACHER[1], ALEXANDER NAUELS[1], AND MALTE MEINSHAUSEN[1,2]

GEOSCIENTIFIC MODEL DEVELOPMENT

[1] Australian-German College of Climate & Energy Transitions, The University of Melbourne, Parkville 3010, Victoria, Australia

[2] The Potsdam Institute for Climate Impact Research, Telegraphenberg A26, 14412 Potsdam, Germany

Table S1: CMIP5 model and scenario ratio of published versus recalculated *zostoga* time-series for the first realisation (*r1i1p1*) marked by "x" if available and "o" if not available; the bottom line sums up the available models and scenarios.

Table S2: Calibration parameters c_n=0-5 for a simplified parameterisation of a thermal expansion coefficient (Equation 3), the sum square error (SSE, in 10^{-4} m2) and the RMS-error normalised by the mean value for each CMIP5 model.

Figure S3: Time series of observed and simulated rate of global mean yearly thSLR (in mm yr-1), cf. Figure 1 in main manuscript. (a/) Simulated thSLR (zostoga) relative to year 1990 for seven CMIP5 scenarios: *historical* (31/47), *1pctCO2* (19/32), *abrupt4xCO2* (17/30), *rcp2.6* (18/26), *rcp4.5* (27/40), *rcp6.0* (13/20), *rcp8.5* (27/40); the ratio in brackets indicates the number of models of published (solid lines) *zostoga* and recalculated (dashed lines) *zostoga* in this study based on simulated temperature and salinity fields. Bars indicate the median and its 90% confidence interval for the projected rate of global mean thSLR (in mm yr^{-1}) of the four RCP-scenarios in year 2100: *rcp2.6* 1.6 [1.1 to 2.2], *rcp4.5* 2.2 [1.7 to 2.7], *rcp6.0* 2.4 [1.9 to 2.9], *rcp8.5* 3.4 [2.7 to 4.2]. (b/) Observed contribution to yearly thSLR of the upper 700 m by Domingues et al. (2008), Ishii and Kimoto (2009) and Levitus et al. (2012) relative to year 1961 and corresponding simulated time series of the *historical* and *rcp4.5* scenarios, whereby the solid light (dark) grey lines represent the model mean (median). Observed contribution to yearly thSLR from layers (c/) between 700-2000 m by *Levitus et al.* (2012) and *Roemmich and Gilson* (2009) and (d/) below 2000 m by *Purkey and Johnson* (2010) relative to year 1993 (indicating the start of the satellite sea level altimetry period). Corresponding simulated time series are shown as in (b/).

Table S4.1: Median and its 90% confidence interval for the constant of proportionality between thermosteric sea level rise (thSLR) and ocean heat uptake (OHU) (in m YJ^{-1}, 1YJ = 10^{24} J) for different depths intervals for the four RCP scenarios, as well as the historical scenario and the two idealized CO_2-forcing scenarios. Based on the ensemble of 30%-less CMIP5 models than used here, the constant for global mean (0-D) time series estimated by Kuhlbrodt and Gregory (2012) for *1pctCO2* amounts to 0.11±0.01 m YJ^{-1}.

Table S4.2: Median and its 90% confidence interval for the constant of proportionality between thSLR and OHU (in m YJ^{-1}, $1YJ = 10^{24}$ J) for different depths intervals for the four RCP scenarios, as well as the historical scenario and the two idealized CO_2-forcing scenarios. Based on the ensemble of 30%-less CMIP5 models than used here, the constant for global mean (0d) time series estimated by Kuhlbrodt and Gregory (2012) for *1pctCO2* amounts to 0.11±0.01 m YJ^{-1}.

Table S5: CMIP5 multi-model mean depth and standard deviation (in 10^{-3} m) where the individual model mean and median depth of thSLR originates for the four RCP scenarios, as well as the *historical* scenario and the two idealized CO_2-forcing scenarios. Averaged over the four RCP scenarios, the global multi-model median depth is 490±90 m, with the range indicating scenario-to-scenario variations.

Table S1: CMIP5 model and scenario ratio of published versus recalculated *zostoga* time-series for the first realisation (*r1i1p1*) marked by "x" if available and "o" if not available; the bottom line sums up the available models and scenarios.

Model Name	Institutional ID, Country	Scenario							
		piControl	historical	1pctCO2	abrupt4xCO2	rcp2.6	rcp4.5	rcp6.0	rcp8.5
ACCESS1-0	CSIRO-BOM, Australia	x/x	x/x	x/x	x/x	o/o	x/x	o/o	x/x
ACCESS1-3		x/x	x/x	x/x	x/x	o/o	x/x	o/o	x/x
BNU-ESM	BCC, China	o/x	o/x	o/x	o/x	o/x	o/x	o/o	o/x
CCSM4	NCAR, USA	x/x	x/x	o/x	o/x	x/x	x/x	x/x	x/x
CESM1-BGC	NSF-DOE-NCAR, USA	o/x	o/x	o/x	o/o	o/o	o/x	o/o	o/x
CESM1-CAM5		o/x	o/x	o/x	o/o	o/x	o/x	o/x	o/x
CESM1-CAM5-FV2		o/x	o/x	o/o	o/o	o/o	o/o	o/o	o/o
CESM1-FASTCHEM		o/x	o/x	o/o	o/o	o/o	o/o	o/o	o/o
CESM1-WACCM		o/x	o/x	o/o	o/o	o/o	o/o	o/o	o/o
CMCC-CESM	CMCC, Italy	x/x	x/x	o/o	o/o	o/o	o/o	o/o	x/x
CMCC-CM		x/x	x/x	o/o	o/o	o/o	x/x	o/o	x/x
CMCC-CMS		x/x	x/x	o/o	o/o	o/o	x/x	o/o	x/x
CNRM-CM5	CNRM-CERFACS, France	x/x	x/x	x/x	x/x	x/x	x/x	o/o	x/x
CNRM-CM5-2		x/x	x/x	x/x	x/x	o/o	o/o	o/o	o/o
CSIRO-Mk3-6-0	CSIRO-QCCCE, Australia	x/x	x/x	x/x	x/x	x/x	x/x	x/x	x/x
CanCM4*	CCCMA, Canada	o/o	x/o	o/o	o/o	o/o	x/o	o/o	o/o
CanESM2		x/x	x/x	x/x	x/x	x/x	x/x	o/o	x/x
EC-EARTH	EC-EARTH, Europe	o/x	o/x	o/o	o/x	o/o	o/x	o/o	o/x
FGOALS-g2	LASG-CESS, China	o/x	o/x	o/x	o/x	o/x	o/x	o/o	o/x
FGOALS-s2	LASG-IAP, China	o/x	o/o	o/x	o/x	o/o	o/o	o/o	o/o
FIO-ESM	FIO, China	o/x	o/x	o/o	o/o	o/o	o/x	o/x	o/x
GFDL-CM2p1	NOAA GFDL, USA	o/o	o/x	o/o	o/o	o/o	o/x	o/o	o/o
GFDL-CM3		o/x	o/x	o/x	o/x	o/x	o/x	o/x	o/x
GFDL-ESM2G		o/x	o/x	o/x	o/x	o/x	o/x	o/x	o/x
GFDL-ESM2M		o/x	o/x	o/x	o/x	o/x	o/x	o/x	o/x
GISS-E2-H	NASA GISS, USA	o/x	o/x	o/x	o/x	o/x	o/x	o/x	o/x
GISS-E2-H-CC		o/x	o/x	o/o	o/o	o/o	o/x	o/o	o/x
GISS-E2-R		x/x	x/x	x/x	x/x	x/x	x/x	x/x	x/x
GISS-E2-R-CC		x/x	x/x	o/o	o/o	o/o	x/x	o/o	x/x
HadGEM2-AO	NIMR/KMA, Korea	o/o	o/x	o/o	o/o	o/x	o/x	o/x	o/x
HadCM3	MOHC, UK	o/o	o/x	o/o	o/o	o/o	o/x	o/o	o/o
HadGEM2-CC		x/x	x/x	o/o	o/o	o/o	x/x	o/o	x/x
HadGEM2-ES		x/x	x/x	x/x	x/x	x/x	x/x	x/x	x/x
IPSL-CM5A-LR	IPSL, France	x/x	x/x	x/x	x/x	x/x	x/x	x/x	x/x
IPSL-CM5A-MR		x/x	x/x	x/x	x/x	x/x	x/x	o/o	x/x
IPSL-CM5B-LR		o/x	o/x	o/x	o/x	o/o	o/x	o/o	o/x
MIROC-ESM	MIROC, Japan	x/x	x/x	x/x	x/x	x/x	x/x	x/x	x/x
MIROC-ESM-CHEM		x/x	x/x	o/o	o/o	x/x	x/x	x/x	x/x
MIROC4h*	MIROC, Japan	x/o	x/o	o/o	o/o	o/o	x/o	o/o	o/o
MIROC5		x/x	x/x	x/x	x/x	x/x	x/x	x/x	x/x
MPI-ESM-LR	MPI, Germany	x/x	x/x	o/x	o/x	x/x	x/x	o/o	x/x
MPI-ESM-MR		x/x	x/x	x/x	x/x	x/x	x/x	o/o	x/x
MPI-ESM-P		x/x	x/x	o/x	o/x	o/o	o/o	o/o	o/o
MRI-CGCM3	MRI, Japan	x/x	x/x	x/x	x/x	x/x	x/x	x/x	x/x
MRI-ESM1		o/o	x/x	o/o	o/o	o/o	o/o	o/o	x/x
NorESM1-M	NCC, Norway	x/x	x/x	x/x	x/x	x/x	x/x	x/x	x/x
NorESM1-ME		x/x	x/x	x/x	o/o	x/x	x/x	x/x	x/x
bcc-csm1-1	BCC, China	x/x	x/x	x/x	x/x	x/x	x/x	x/x	x/x
bcc-csm1-1-m		x/x	x/x	x/x	x/x	x/x	x/x	x/x	x/x
inmcm4	INM, Russia	x/x	x/x	x/x	x/x	o/o	x/x	o/o	x/x
=50		=29/44	=31/47	=19/32	=18/30	=18/26	=27/40	=13/20	=27/40

Table S2: Calibration parameters $c_{n=0-5}$ for a simplified parameterisation of a thermal expansion coefficient (Equation 3), the sum square error (SSE, in 10^{-4} m^2) and the RMS-error normalised by the mean value for each CMIP5 model.

Model Name	Institute ID, Country	Calibration Parameter						SSE	NRMSE
		c0	c1	c2	c3	c4	c5		
ACCESS1-0	CSIRO-BOM, Australia	66.1702	0.8605	0.7033	0.1815	13.6618	0.5000	0.1392	4.3
ACCESS1-3		68.1256	0.8722	0.6865	0.1381	16.7512	0.5000	0.1555	6.7
BNU-ESM	BCC, China	30.0051	1.0907	1.2127	0.7510	39.5652	0.5001	0.1665	3.2
CCSM4	NCAR, USA	69.9441	0.7312	0.3998	0.0002	15.3485	0.7325	0.7839	6.0
CESM1-BGC		52.5531	0.8957	0.5328	0.0000	29.7846	0.5921	0.0320	2.1
CESM1-CAM5		63.1768	0.7830	0.6291	1.1275	29.7090	0.7334	0.1393	3.7
CESM1-CAM5-FV2	NSF-DOE-NCAR,	39.7108	1.5778	2.9999	0.9958	30.5517	0.5108	0.0034	17.4
CESM1-FASTCHEM	USA	39.6641	0.8436	0.0001	0.5658	39.8165	1.3393	0.0024	13.9
CESM1-WACCM		36.6208	1.1734	1.3799	0.8162	35.1718	0.8216	0.0054	7.9
CMCC-CESM		69.3446	0.8489	0.4933	0.0000	14.0680	0.8307	0.0285	7.9
CMCC-CM	CMCC, Italy	30.0023	1.0390	0.6318	0.0000	33.6252	0.9716	0.0240	12.1
CMCC-CMS		52.1939	0.9058	0.4987	0.0001	26.8729	0.8547	0.0258	8.5
CNRM-CM5	CNRM-CERFACS, France	69.3351	0.8441	1.0471	1.0217	19.9257	0.5001	0.2426	3.5
CNRM-CM5-2		52.3706	0.9451	1.0488	1.0021	28.3298	0.7120	0.0277	2.5
CSIRO-Mk3-6-0	CSIRO-QCCCE, Australia	69.9610	0.9178	1.3079	1.2883	10.0077	1.2572	0.8315	7.9
CanCM4*	CCCMA, Canada								
CanESM2		69.9999	0.8280	0.8679	1.1307	21.3029	0.8229	0.2138	3.2
EC-EARTH	EC-EARTH, Europe	70.0000	0.7342	0.4040	0.0713	14.8863	0.8092	0.2310	6.2
FGOALS-g2	LASG-CESS, China	69.9993	0.7559	0.4361	0.1533	20.4448	0.5038	0.1876	5.3
FGOALS-s2	LASG-IAP, China	37.6139	1.7678	4.3999	0.0294	10.0031	0.5942	2.0764	3.5
FIO-ESM	FIO, China	60.7810	0.8378	0.4299	1.1377	28.2507	0.5000	0.0679	4.0
GFDL-CM2p1	NOAA GFDL, USA	30.0014	1.1294	0.7981	0.5789	37.4192	0.8222	0.0095	1.4
GFDL-CM3		30.0197	1.1468	1.4562	0.8966	34.2579	0.7782	0.3463	1.9
GFDL-ESM2G		55.8202	0.7884	0.0000	0.0032	29.5297	0.9572	0.2706	6.1
GFDL-ESM2M		69.9987	0.7611	0.4611	1.2639	23.6699	0.6449	0.2392	4.7
GISS-E2-H		51.7110	0.9696	1.0742	0.9169	29.9094	0.5000	0.0857	1.4
GISS-E2-H-CC	NASA GISS, USA	58.5366	0.8919	0.5885	0.0002	27.6031	0.8345	0.1130	2.0
GISS-E2-R		47.4595	0.8359	0.5737	1.7317	36.2305	0.5000	0.1997	1.8
GISS-E2-R-CC		30.0006	0.9669	0.4508	1.2973	38.4042	0.8826	0.0127	2.2
HadGEM2-AO	NIMR/KMA, Korea	50.2025	1.0094	0.9756	0.0001	28.7180	0.5000	0.0476	1.7
HadCM3		53.5790	1.1204	1.4739	1.7653	10.0011	0.7202	0.0033	10.9
HadGEM2-CC	MOHC, UK	34.2930	1.2163	1.5412	0.0001	27.3219	0.8059	0.0344	4.4
HadGEM2-ES		48.5214	1.0168	1.3568	0.8059	27.6046	0.7220	0.5273	3.3
IPSL-CM5A-LR		60.9507	1.0268	1.3431	0.6023	10.0016	0.6614	0.7052	7.2
IPSL-CM5A-MR	IPSL, France	51.7415	1.0234	0.8728	0.0000	14.2141	0.5001	0.1571	7.5
IPSL-CM5B-LR		69.9999	0.8012	0.6998	1.0521	18.5821	0.5239	0.0645	2.2
MIROC-ESM	MIROC, Japan	48.9823	0.9760	0.9837	0.4033	28.5333	0.5000	0.1891	0.7
MIROC-ESM-CHEM		41.7726	1.0653	1.0743	0.0000	30.9971	0.5432	0.0627	0.8
MIROC4h*	MIROC, Japan								
MIROC5		56.0653	0.8923	0.6888	0.8731	10.0000	1.6042	0.1815	7.0
MPI-ESM-LR		41.9764	1.5536	3.0000	1.6868	21.5158	1.8395	3.2266	3.1
MPI-ESM-MR	MPI, Germany	69.9994	0.9777	1.1201	0.3959	12.1619	0.7649	0.3062	8.0
MPI-ESM-P		47.6048	1.5670	2.7601	0.1597	10.0022	0.6843	0.4684	3.0
MRI-CGCM3	MRI, Japan	69.7154	0.8299	0.5622	0.0003	10.0001	0.5541	0.0751	3.2
MRI-ESM1		32.2583	1.1082	1.3472	1.3510	30.0966	0.5000	0.0237	3.9
NorESM1-M	NCC, Norway	30.0007	1.1634	1.2557	0.2615	35.2126	0.8209	0.1405	2.0
NorESM1-ME		30.0004	1.2486	1.4890	0.1635	33.6798	0.6718	0.0571	1.2
bcc-csm1-1	BCC, China	68.9957	0.7696	0.4575	0.0000	10.0001	0.6921	0.4283	8.1
bcc-csm1-1-m		39.9433	1.0834	1.0867	0.0000	21.0694	0.9437	0.0836	3.7
inmcm4	INM, Russia	69.6425	0.5120	0.0002	2.4906	39.8744	0.5002	0.6116	12.3
=50		52.2368	0.9938	1.0333	0.6065	24.2643	0.7408	0.2928	5.1

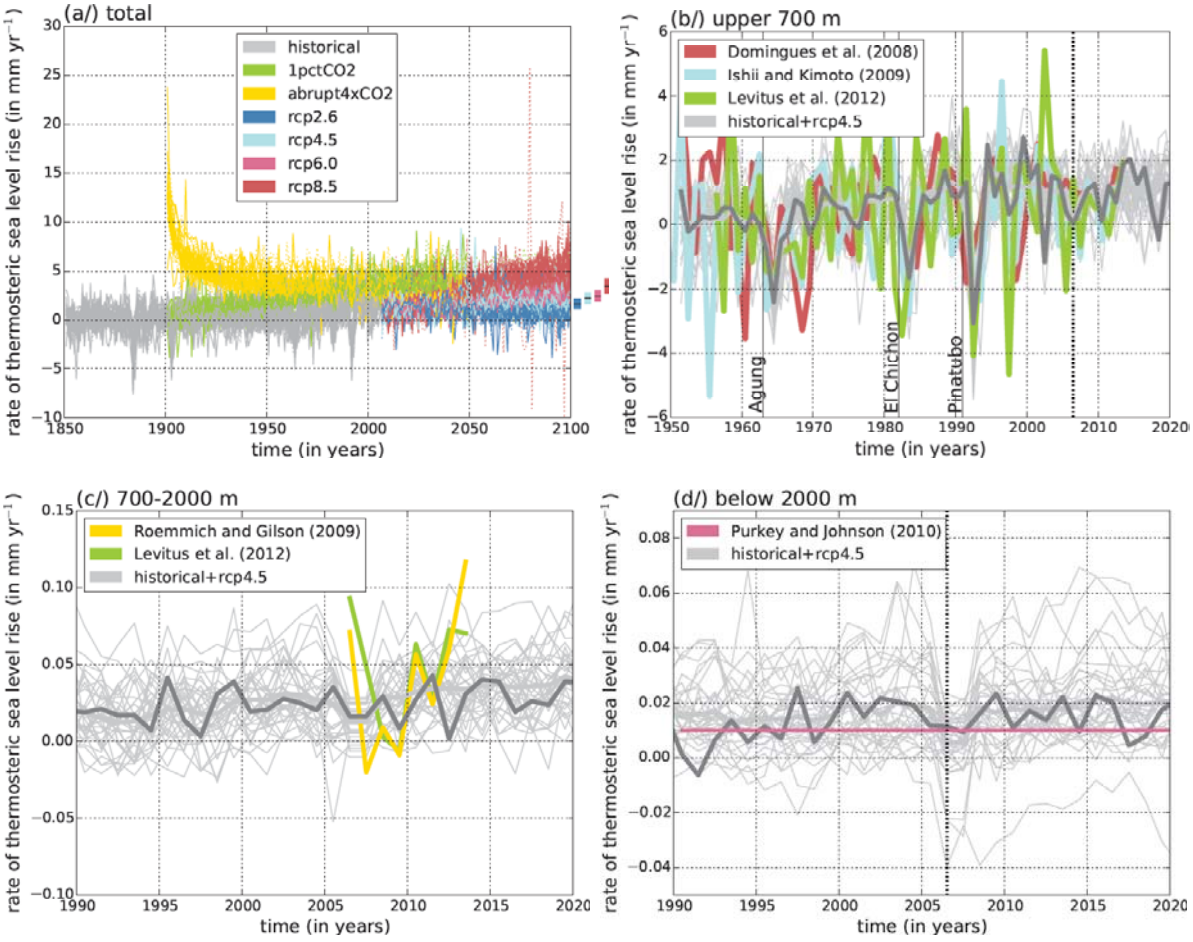

Figure S3: Time series of observed and simulated rate of global mean yearly thSLR (in mm yr-1), cf. Figure 1 in main manuscript. (a/) Simulated thSLR (zostoga) relative to year 1990 for seven CMIP5 scenarios: *historical* (31/47), *1pctCO2* (19/32), *abrupt4xCO2* (17/30), *rcp2.6* (18/26), *rcp4.5* (27/40), *rcp6.0* (13/20), *rcp8.5* (27/40); the ratio in brackets indicates the number of models of published (solid lines) *zostoga* and recalculated (dashed lines) *zostoga* in this study based on simulated temperature and salinity fields. Bars indicate the median and its 90% confidence interval for the projected rate of global mean thSLR (in mm yr^{-1}) of the four RCP-scenarios in year 2100: *rcp2.6* 1.6 [1.1 to 2.2], *rcp4.5* 2.2 [1.7 to 2.7], *rcp6.0* 2.4 [1.9 to 2.9], *rcp8.5* 3.4 [2.7 to 4.2]. (b/) Observed contribution to yearly thSLR of the upper 700 m by Domingues et al. (2008), Ishii and Kimoto (2009) and Levitus et al. (2012) relative to year 1961 and corresponding simulated time series of the *historical* and *rcp4.5* scenarios, whereby the solid light (dark) grey lines represent the model mean (median). Observed contribution to yearly thSLR from layers (c/) between 700-2000 m by *Levitus et al.* (2012) and *Roemmich and Gilson* (2009) and (d/) below 2000 m by *Purkey and Johnson* (2010) relative to year 1993 (indicating the start of the satellite sea level altimetry period). Corresponding simulated time series are shown as in (b/).

Table S4.1: Median and its 90% confidence interval for the constant of proportionality between thermosteric sea level rise (thSLR) and ocean heat uptake (OHU) (in m YJ^{-1}, $1YJ \equiv 10^{24}$ J) for different depths intervals for the four RCP scenarios, as well as the historical scenario and the two idealized CO_2-forcing scenarios. Based on the ensemble of 30%-less CMIP5 models than used here, the constant for global mean (0-D) time series estimated by Kuhlbrodt and Gregory (2012) for *1pctCO2* amounts to 0.11±0.01 m YJ^{-1}.

scenario		rcp8.5	rcp6.0	rcp4.5	rcp2.6	historical	1pctCO2	abrupt4xCO2
period		2006-2100	2006-2100	2006-2100	2006-2100	1900-2005	1-100	1-100
epsilon (constant of proportionality)	total	0.12 [0.11 to 0.13]	0.12 [0.10 to 0.13]	0.12 [0.10 to 0.13]	0.11 [0.09 to 0.12]	0.12 [0.11 to 0.14]	0.12 [0.11 to 0.13]	0.12 [0.11 to 0.13]
	upper 700m	0.14 [0.13 to 0.15]	0.13 [0.13 to 0.14]	0.13 [0.12 to 0.14]	0.13 [0.12 to 0.14]	0.14 [0.13 to 0.15]	0.13 [0.13 to 0.14]	0.14 [0.13 to 0.14]
	upper 700-2000m	0.09 [0.08 to 0.11]	0.09 [0.08 to 0.10]	0.09 [0.08 to 0.11]	0.09 [0.08 to 0.11]	0.09 [0.08 to 0.11]	0.09 [0.08 to 0.10]	0.10 [0.08 to 0.11]
	below 700m	0.10 [0.08 to 0.10]	0.10 [0.08 to 0.10]	0.10 [0.09 to 0.11]	0.10 [0.08 to 0.11]	0.09 [0.08 to 0.11]	0.09 [0.09 to 0.10]	0.10 [0.08 to 0.11]
	below 2000m	0.10 [0.09 to 0.11]	0.10 [0.09 to 0.11]	0.10 [0.09 to 0.11]	0.10 [0.09 to 0.11]	0.10 [0.08 to 0.12]	0.10 [0.09 to 0.11]	0.10 [0.09 to 0.11]

Table S4.2: Median and its 90% confidence interval for the constant of proportionality between thSLR and OHU (in m YJ^{-1}, 1YJ = 10^{24} J) for different depths intervals for the four RCP scenarios, as well as the historical scenario and the two idealized CO_2-forcing scenarios. Based on the ensemble of 30%-less CMIP5 models than used here, the constant for global mean (0d) time series estimated by Kuhlbrodt and Gregory (2012) for *1pctCO2* amounts to 0.11±0.01 m YJ^{-1}.

	scenario	rcp8.5	rcp6.0	rcp4.5	rcp2.6	historical	1pctCO2	abrupt4xCO2
model name	period	2006-2100	2006-2100	2006-2100	2006-2100	1900-2005	1-100	1-100
ACCESS1-0		0.13	—	0.12	—	0.12	0.12	0.12
ACCESS1-3		0.13	—	0.12	0.10	0.13	0.13	0.12
BNU-ESM		0.12	—	0.11	0.11	0.12	0.12	0.12
CCSM4		0.16	0.11	0.11	0.10	0.12	0.12	0.11
CESM1-BGC		0.12	—	0.11	0.00	0.12	0.12	—
CESM1-CAM5		0.12	0.12	0.11	0.11	0.12	0.12	—
CESM1-CAM5-FV2		—	—	—	—	0.12	—	—
CESM1-FASTCHEM		—	—	—	—	0.12	—	—
CESM1-WACCM		—	—	—	—	0.12	—	—
CMCC-CESM		0.12	—	—	—	0.11	—	—
CMCC-CM		0.12	—	0.12	—	0.13	—	—
CMCC-CMS		—	—	—	—		—	—
CNRM-CM5		0.13	—	0.12	—	0.13	—	—
CNRM-CM5-2		0.12	—	0.12	0.11	0.12	0.12	0.12
CSIRO-Mk3-6-0		0.13	0.12	0.12	0.12	0.14	0.13	0.13
CanCM4*		—	—	—	—		—	—
CanESM2		0.13	—	0.12	0.11	0.14	0.13	0.13
EC-EARTH		0.12	—	0.11	—	0.12	0.12	0.12
FGOALS-g2		0.11	—	0.10	0.10	0.13	0.13	0.12
FGOALS-s2		—	—	—	—	—	0.13	0.16
FIO-ESM		0.13	0.12	0.11	—	0.12	—	—
GFDL-CM2p1		—	—	0.11	—	0.13	—	—
GFDL-CM3		0.13	0.12	0.12	0.12	0.13	0.12	0.13
GFDL-ESM2G		0.11	0.11	0.10	0.10	0.12	0.10	0.13
GFDL-ESM2M		—	—	—	—	—		—
GISS-E2-H		0.12	0.11	0.11	0.11	0.11	0.12	0.11
GISS-E2-H-CC		0.12	—	0.11	—	0.13		—
GISS-E2-R		0.12	0.13	0.12	0.11	0.12	0.13	0.12
GISS-E2-R-CC		—	—	—	—	—	—	—
HadGEM2-AO		0.12	0.12	0.11	0.11	0.12	—	—
HadCM3		—	—	0.12	—	0.14	—	—
HadGEM2-CC		0.12	—	0.11	—	0.12	—	—
HadGEM2-ES		0.12	0.12	0.11	0.11	0.13	0.12	0.12
IPSL-CM5A-LR		0.12	0.11	0.11	0.11	0.13	0.12	0.12
IPSL-CM5A-MR		0.12	—	0.11	0.10	0.11	0.12	0.12
IPSL-CM5B-LR		0.13	—	0.12	—	0.11	0.12	0.12
MIROC-ESM		0.12	0.12	0.11	0.11	0.11	0.11	0.12
MIROC-ESM-CHEM		0.12	0.12	0.11	0.11	0.11	—	—
MIROC4h*		—	—	—	—	—	—	—
MIROC5		0.12	0.12	0.11	0.11	0.13	0.12	0.11
MPI-ESM-LR		0.12	—	0.11	0.11	0.11	0.13	0.12
MPI-ESM-MR		0.12	—	0.12	0.11	0.12	0.12	0.12
MPI-ESM-P		—	—	—	—	0.12	0.12	0.12
MRI-CGCM3		0.13	0.12	0.12	0.12	0.12	0.12	0.12
MRI-ESM1		0.13	—	—	—	0.13	—	—
NorESM1-M		0.12	0.11	0.11	0.10	0.12	0.11	0.11
NorESM1-ME		0.11	0.11	0.11	0.10	0.12	0.11	—
bcc-csm1-1		0.12	0.12	0.12	0.18	0.12	0.12	0.12
bcc-csm1-1-m		0.12	0.12	0.11	0.11	0.13	0.12	0.12
inmcm4		0.13	—	0.12	—	0.13	0.13	0.13
=50		0.12	0.12	0.11	0.11	0.12	0.12	0.12

Table S5: CMIP5 multi-model mean depth and standard deviation (in 10^{-3} m) where the individual model mean and median depth of thSLR originates for the four RCP scenarios, as well as the *historical* scenario and the two idealized CO_2-forcing scenarios. Averaged over the four RCP scenarios, the global multi-model median depth is 490±90 m, with the range indicating scenario-to-scenario variations.

scenario		rcp8.5	rcp6.0	rcp4.5	rcp2.6	historical	1pctCO2	abrupt4xCO2
period		2081-2100	2081-2100	2081-2100	2081-2100	1986-2005	81-100	81-100
global	mean	0.70 ±0.18	0.83 ±0.22	0.84 ±0.22	0.95 ±0.29	0.99 ±0.43	0.44 ±0.11	0.57 ±0.11
	median	0.40 ±0.15	0.47 ±0.15	0.52 ±0.18	0.59 ±0.23	0.57 ±0.44	0.39 ±0.11	0.50 ±0.10
northern hemisphere	mean	0.61 ±0.14	0.72 ±0.15	0.73 ±0.17	0.83 ±0.25	0.99 ±0.50	0.37 ±0.10	0.50 ±0.09
	median	0.38 ±0.14	0.44 ±0.13	0.49 ±0.16	0.58 ±0.21	0.67 ±0.57	0.37 ±0.11	0.48 ±0.09
southern hemisphere	mean	0.80 ±0.22	0.96 ±0.28	0.96 ±0.28	1.07 ±0.34	1.04 ±0.39	0.52 ±0.14	0.65 ±0.14
	median	0.42 ±0.18	0.51 ±0.18	0.56 ±0.22	0.68 ±0.26	0.58 ±0.40	0.42 ±0.14	0.53 ±0.12